Bismuth-stabilized (2×1) and (2×4) reconstructions on GaAs(100) surfaces: Combined first-principles, photoemission, and scanning tunneling microscopy study

M. P. J. Punkkinen,[1,*] P. Laukkanen,[1,2,†] H.-P. Komsa,[3] M. Ahola-Tuomi,[1] N. Räsänen,[1] K. Kokko,[1] M. Kuzmin,[1] J. Adell,[4] J. Sadowski,[4,5] R. E. Perälä,[1] M. Ropo,[6] T. T. Rantala,[3] I. J. Väyrynen,[1] M. Pessa,[2] L. Vitos,[7,8,9] J. Kollár,[9] S. Mirbt,[8] and B. Johansson[7,8,10]

[1]*Department of Physics, University of Turku, FI-20014 Turku, Finland*
[2]*Optoelectronics Research Centre, Tampere University of Technology, FI-33101 Tampere, Finland*
[3]*Department of Physics, Tampere University of Technology, FI-33101 Tampere, Finland*
[4]*Department of Applied Physics, Chalmers University of Technology, SE-41296 Göteborg, Sweden and MAX-lab, Lund University, SE-221 00 Lund, Sweden*
[5]*Institute of Physics, Polish Academy of Sciences, al. Lotnikow 32/46, 02-668 Warszawa, Poland*
[6]*Department of Information Technology, Åbo Akademi University, FI-20500 Turku, Finland*
[7]*Department of Materials Science and Engineering, Applied Materials Physics, Royal Institute of Technology, SE-10044 Stockholm, Sweden*
[8]*Department of Physics and Materials Science, Division for Materials Theory, Uppsala University, SE-75121 Uppsala, Sweden*
[9]*Research Institute for Solid State Physics and Optics, P.O. Box 49, H-1525 Budapest, Hungary*
[10]*School of Physics and Optoelectronic Technology and College of Advanced Science and Technology, Dalian University of Technology, Dalian 116024, China*

(Received 11 July 2008; revised manuscript received 15 September 2008; published 4 November 2008)

Bismuth adsorbate-stabilized (2×1) and (2×4) reconstructions of the GaAs(100) surfaces have been studied by first-principles calculations, valence-band and core-level photoelectron spectroscopies, and scanning tunneling microscopy. It is demonstrated that large Bi atom size leads to the formation of the pseudogap at the Fermi energy and to the lower energy of an adsorbate-derived surface band, which contributes to the stabilization of the exceptional Bi/GaAs(100)(2×1) reconstruction. It is proposed that the Bi/GaAs(100)(2×4) reconstructions include asymmetric mixed Bi-As dimers, in addition to the Bi-Bi dimers. Based on the calculations, we solve the atomic origins of the surface core-level shifts (SCLSs) of the Bi 5*d* photoemission spectra from the Bi/GaAs(100)(2×4) surfaces. This allows for resolving the puzzle related to the identification of two SCLS components often found in the measurements of the Bi 5*d* and Sb 4*d* core-level emissions of the Bi/III-V and Sb/III-V(100)(2×4) surfaces. Finally, the reason for the absence of the common (2×4)-β2 structure and additional support for the stability of the (2×1) structure on the Bi/III-V(100) surfaces are discussed in terms of Bi atom size and subsurface stress.

DOI: 10.1103/PhysRevB.78.195304 PACS number(s): 68.35.−p, 81.10.−h, 73.20.−r

I. INTRODUCTION

The group V adsorbate bismuth (Bi) has been increasingly used in the epitaxial growth of III-V electronics materials, which is essentially a surface process proceeding via group V stabilized III-V(100) reconstructions. In particular, Bi has been utilized as a surfactant[1–3] in the growth and also alloyed with III-V's (e.g., $GaAs_{1-x}Bi_x$) to produce optoelectronic and spintronic materials.[4–6] In order to realize the growth process of the Bi alloys and to understand why the presence of the Bi surfactant on the growing surface improves the characteristics of device materials (e.g., leads to smoother interfaces and higher photoluminescence intensity),[2,3] it is crucial to understand the fundamental properties of the Bi-stabilized III-V(100) surfaces.

The Bi/III-V(100) surfaces have recently been found to behave differently from other group V stabilized III-V(100) surfaces such as As/GaAs(100) and Sb/GaAs(100),[7–10] which might be related to the above mentioned advantageous Bi surfactant effects. First, Bi has been found to stabilize an unusual (2×1) reconstruction.[7–10] Such system should be metallic and unstable according to the electron counting model (ECM),[11–13] which has been successfully used to explain various reconstructions of III-V's. Recently, we showed that these Bi/III-V(100)(2×1) surfaces are stabilized by stress relief and pseudogap formation.[10] Figs. 1(a)–1(c) present the recently found atomic models,[10] which are energetically favored and hitherto explain the measurements of both metallic and semiconducting Bi/III-V(100)(2×1) phases. Indeed, the Bi-stabilized (2×1) growth front might lead to the improved III-V interfaces in the surfactant growth[2,3] because the III atom diffusion should increase on the metallic (2×1) surface,[14] which has also an atomically

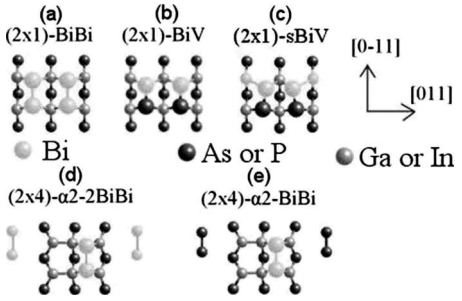

FIG. 1. Atomic models for the Bi/III-V-(2×1) and −(2×4)-α2 surfaces.

smoother contour than a (2×4) reconstruction, usually observed during the growth. The second specific property of Bi is that it favors a (2×4)-$\alpha2$ reconstruction rather than the common (2×4)-$\beta2$, which[15–25] has been found on several III-V(100) surfaces. A reason for that has remained unclear. A prerequisite for understanding the mechanism behind this phenomenon is the detailed knowledge of the atomic and electronic structures of the Bi/III-V(100)(2×4)-$\alpha2$ reconstructions.

The object of this work is to complement substantially the picture presented in our recent publication.[10] Here we present additional photoemission data combined with the first-principles calculations, which support the recently proposed (2×1) structural models and stabilizing mechanisms responsible for the formation of this peculiar (2×1) reconstruction. Especially, the formation of the pseudogap at the Fermi energy is demonstrated by theoretical band structures and density-of-states (DOS) curves. Furthermore, it is proposed, combining total-energy calculations, calculated and measured scanning tunneling microscopy (STM) results, and core-level photoemission results, that the Bi/GaAs(100)(2×4)-$\alpha2$ surface includes asymmetric mixed Bi-As dimers, in addition to symmetric Bi-Bi dimers. We solve the atomic origins of surface core-level shifts (SCLSs) in the photoemission spectra from the Bi/III-V(100)(2×4) surfaces. In particular, the results allow for resolving the puzzle related to the atomic origins of two SCLS components found in the measurements of Bi $5d$ and Sb $4d$ core-level emissions of the Bi/III-V and Sb/III-V(100)(2×4).[7,26–28] Our calculated data allow us also to complement our previous discussion of the stability of the (2×4) and (2×1) reconstructions.

This paper is organized as follows. First, we present data from our valence-band photoemission measurements of the Bi/GaAs(100)(2×1) surface and from our *ab initio* band-structure calculations. Next, the measured and calculated core-level and STM results are presented and interpreted for the Bi/GaAs(100)(2×4) surface. Finally, the relative stabilities of the Bi/III-V(100)(2×4)-$\alpha2$, $-(2\times4)$-$\beta2$, and $-(2\times1)$ are discussed using theoretical results.

II. EXPERIMENTS

The synchrotron radiation photoelectron spectroscopy measurements were done at room temperature (RT) in ultrahigh vacuum (UHV) at the MAX-laboratory (beamline 41) in Sweden using an angle-resolving analyzer with an acceptance angle of about 2°. The incident-beam angle was 45° relative to the surface. Instrumental energy resolution was 0.15–0.35 eV depending on the photon energy used. The Fermi level was obtained from a spectrum of the Ta plate connected to the sample holder. The Fermi energy was determined as the minimum of its derivative spectrum around the Fermi step of the Ta plate.

An undoped GaAs buffer layer (100 nm) was grown on an n-type ($\sim10^{18}$ cm^{-3}) GaAs(100) substrate by a molecular beam epitaxy (MBE) equipment, connected to the photoemission chamber, and transferred under UHV into the photoemission chamber. The substrate was heated around 570 °C until a sharp (6×6) LEED pattern was seen. Also, the (4×2) pattern was found locally on this substrate. Then 1–1.5 ML of Bi was deposited on the substrate kept at RT. When the Bi/GaAs was heated at 270 °C (4 h), a clear (2×1) LEED pattern without any other phase was seen. Heating around 370 °C produced the Bi/GaAs(100)(2×4) surface.

For the RT-STM measurements (constant current mode) at a separate UHV system, a GaAs(100) substrate was cut from the n-type ($\sim10^{18}$ cm^{-3}) wafer. It was cleaned by argon ion sputtering (1 keV and 10 mA). During the 0.5 h sputtering, the substrate temperature was about 500 °C, and after that it was increased under UHV to 580 °C for 0.5 h. Repeating this cycle four times produced a good-quality GaAs(100)(6×6) substrate with local (4×2) areas, as deduced from STM and low-energy electron diffraction (LEED) measurements. The Bi/GaAs surface was prepared as described above.

III. CALCULATIONAL METHODS

The theoretical calculations were performed using the *ab initio* density-functional total-energy code with the local-density approximation.[29,30] The approach is based on plane-wave basis and projector augmented wave method[31,32] [Vienna *ab initio* simulation package (VASP)].[33–36] The (2×1) and (2×4) reconstructions in Fig. 1 were simulated by (2×4) slabs having 11 atomic layers (+ pseudohydrogen atoms) and keeping all d electrons in the core. Pseudohydrogenated slabs[37] were used with the energy cutoff of 350 eV. Two bottom atomic layers of the slabs were fixed to the ideal positions. Other atoms, including pseudohydrogen atoms, were relaxed until the remaining forces were less than 20 meV/Å. The number of k points in the Brillouin zone was eight corresponding to 64 k points in the (1×1) slab. The band structures of the (2×1) reconstructions were calculated by using (2×1) and (2×2) slabs and several tens of k points in different high-symmetry directions. In these calculations the Ga $3d$ electrons were treated as valence electrons. The DOS curves were calculated by using 288 k points in the Brillouin zone of the (2×1) slab. Smoothing was applied to make the DOS curves more continuous, however, without affecting the major results and conclusions, especially concerning the pseudogap at the Fermi energy, at all. The surface energies were evaluated as a function of chemical potentials (μ) in the standard way. The lattice parameters of the bulk cubic zinc-blende structure were obtained from our calculations: 3.962 Å (Ga $3d$ electrons in the valence) and 3.976 Å (all d electrons in the core). Our tests showed that the inclusion of the Ga $3d$ electrons in the valence does not affect significantly the surface phase diagrams. SCLSs were calculated within the initial state model, which has been shown to give theoretical SCLSs in a quite good agreement with the experimental values for the GaAs(100)(2×4).[38]

IV. RESULTS AND DISCUSSION

A. Band structures and the stabilizing effect

Before considering photoemission results, we recall that three different (2×1) structures, namely, the metallic BiBi

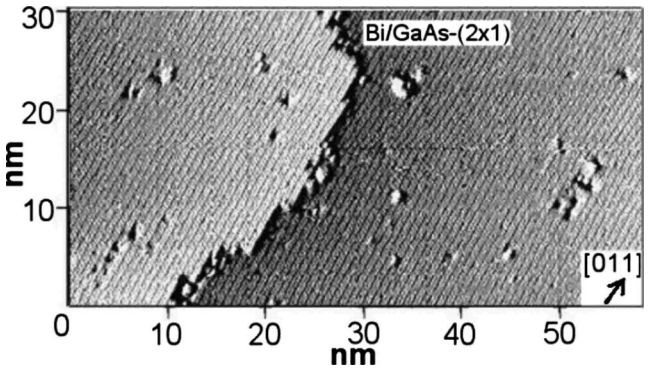

FIG. 2. Filled-state STM image of the Bi/GaAs(100)(2×1); tunneling current I=0.31 nA and voltage V=2.49 V.

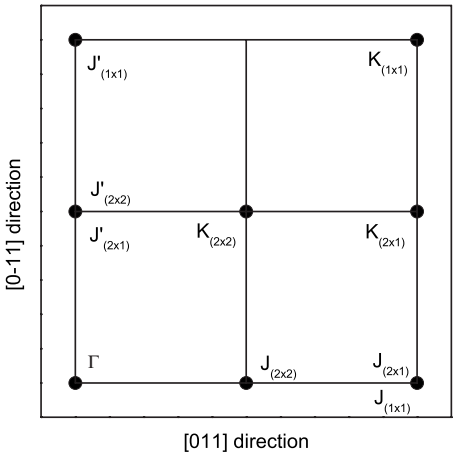

FIG. 4. The special symmetry directions and k points for the square and rectangular irreducible parts of the surface Brillouin zones of the Bi/GaAs(100)(2×1) and Bi/GaAs(100)(2×2) reconstructions.

and BiV phases and semiconducting sBiV one (Fig. 1) were previously identified for the Bi/III-V(100)(2×1) surfaces (Bi/GaAs and Bi/InP).[10] Figure 2 presents a large-scale STM image from the Bi/GaAs(100)(2×1) surface, indicating a reasonable surface quality for the angle-resolved valence-band measurements shown in Fig. 3. The dispersions of distinct emissions (i.e., bulk emission b and surface-related bands $s1$ and $s2$) are mapped along the [0−11] symmetry direction (i.e., Γ-J') from bottom to top in Fig. 3(a). Due to technical problems, we have not been able to measure so far the dispersions of the Bi/GaAs(100)(2×1) in the orthogonal [011] direction (i.e., the Γ-J azimuth). Figure 3(b) shows the zoomed spectra of Fig. 3(a) near the Fermi level and around the normal (0°) emission (i.e., the Γ point). They show a nonzero Fermi-level intensity for the emission angles of 4° and 6°. This Fermi-level intensity is not high, but it is worth to note that the Fermi-level emission is usually completely zero for a semiconducting surface structure. Figure 3(c) gives support to the appearance of the small Fermi-level emission from the Bi/GaAs(100)(2×1) surface. As can be seen, the Fermi-level emission is enhanced in the spectrum measured with higher photon energy, as compared to the spectra in Figs. 3(a) and 3(b). These results indicate the presence of the metallic areas on the Bi/GaAs(100)(2×1) surface, in good agreement with the recent scanning tunneling spectroscopy findings in Ref. 10.

The high-symmetry directions and k points for the square and rectangular irreducible parts of the surface Brillouin zones (SBZ) of the (2×1) and (2×2) reconstructions are shown in the Fig. 4. The [0−11] direction is parallel to the direction of the Bi dimer bond [orthogonal to the direction of Bi dimer rows of the (2×1) reconstruction] (Γ-J'). The BiBi and BiV reconstructions have a rectangular (2×1) SBZ,

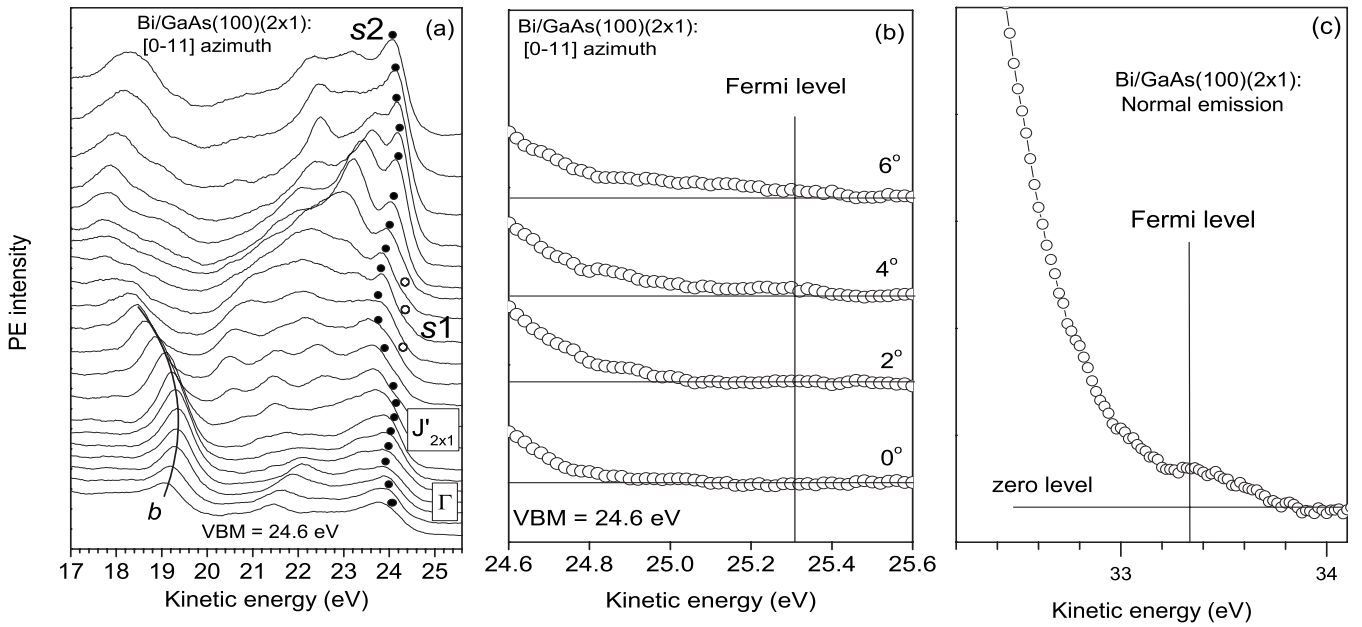

FIG. 3. (a) Valence-band spectra of the Bi/GaAs(100)(2×1) along the [0−11] direction; the photon energy is 30 eV. Dispersions of the surface-related bands $s1$ (open circles) and $s2$ (solid circles) are shown. (b) Zoomed spectra of the Fig. 3(a) near the Fermi energy and around the normal emission. (c) Normal Fermi-level emission from the Bi/GaAs(100)(2×1) surface with the photon energy of 38 eV.

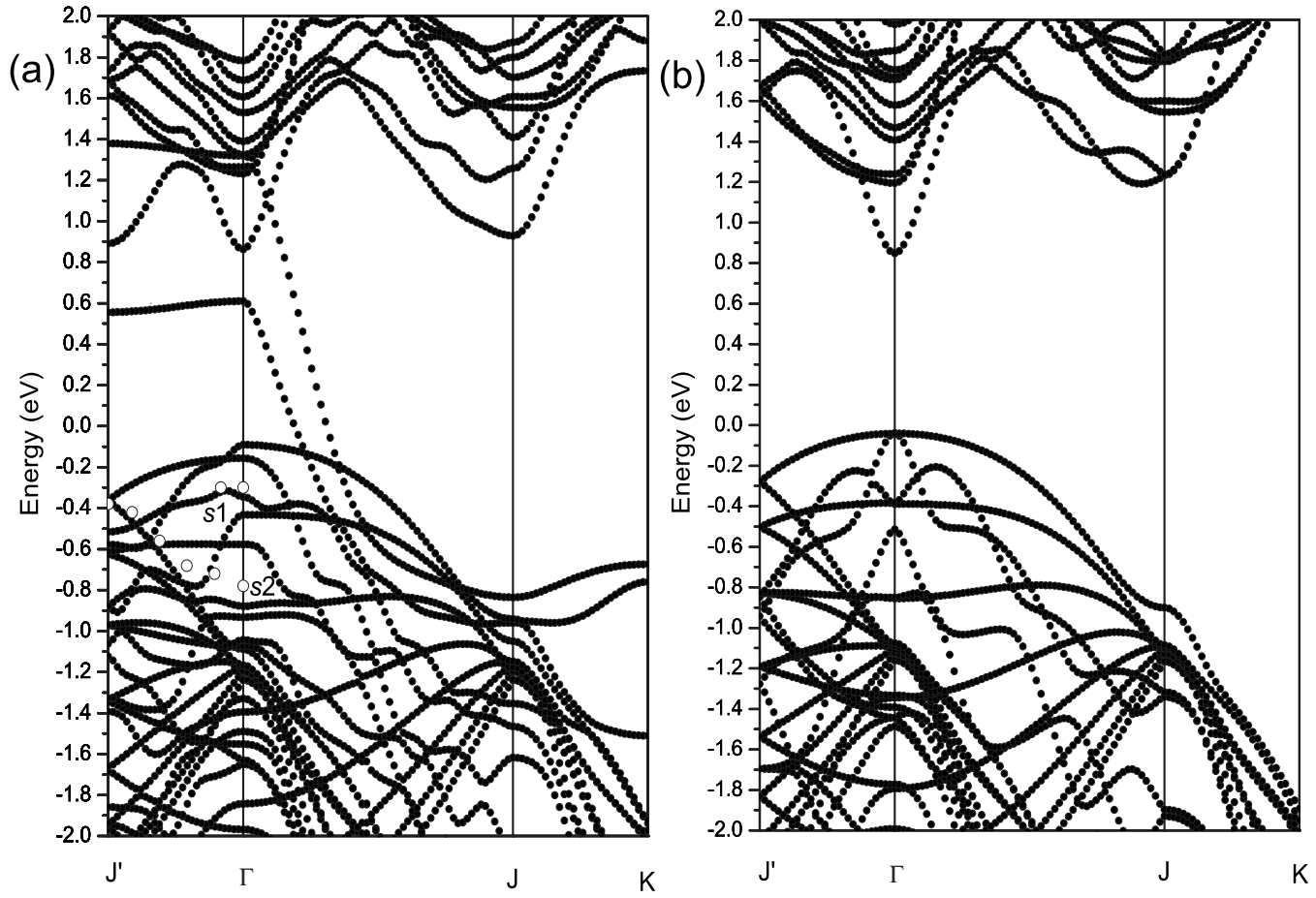

FIG. 5. (a) Theoretical and experimental band structures along the main symmetry directions of the Bi/GaAs(100)(2×1)-BiBi reconstruction. The theoretical Fermi level is set at 0 eV. The solid circles denote the theoretical results, whereas the open circles denote the experimental results. (b) Band structure of the bulk GaAs calculated by pseudohydrogenating the both surfaces of the slab. The 0 eV level is set at the bottom of the energy gap.

whereas the sBiV reconstruction has a square (2×2) SBZ due to the substitutional second layer Bi atom. The calculated band structures along Γ-J', Γ-J, and J-K symmetry directions are shown in Fig. 5(a) for the BiBi and Fig. 6(a) for the sBiAs. Moreover the zero energy is set at the theoretical Fermi energy and at the bottom of the energy gap correspondingly. The corresponding bulk band structure is shown in the Fig. 5(b). This was calculated by pseudohydrogenating both surfaces of the slab, which enables easy comparison between the band structures of the bulk and surface systems, because the states due to pseudohydrogens are included. The band structure of the metallic BiAs reconstruction has similarities with both the BiBi and sBiAs, and it is not shown. The distance between the Γ and J points of the sBiAs is half of the corresponding distance of the BiBi and BiAs. The experimental electron energy-k vector positions of the $s1$ and $s2$, measured along the Γ-J' direction, are also shown in Figs. 5(a) and 6(a) by open circles. These positions are determined by estimating and equating the experimental and theoretical bulk valence-band maxima. The experimentally determined Fermi level is about 0.7 eV above the bulk valence-band maximum (VBM), and the theoretical one is about 0.1 eV above bulk VBM for the metallic (2×1)-BiBi structure. However, one should note that the sample consists of different (2×1) phases including also a semiconducting one (i.e., the sBiAs).[10] Therefore, it is not surprising that the experimental Fermi energy deviates from the theoretical Fermi energy determined for the metallic phases. The Fermi energy for the semiconducting phase is not uniquely determined, and it can be, in principle, at any energy value inside the energy gap. Furthermore, the magnitude of the band gap is underestimated by the local-density approximation for the exchange-correlation functional, as is well known. Additionally, the experimental uncertainties in the Fermi energy and VBM determinations can cause discrepancies. Photoemission measurements probe a much larger surface area than the STM measurements. Comparison with the bulk band structure suggests that these surface-related bands are surface resonances. It is noticed that the agreement between theoretical and experimental data is good. The calculations show that the experimental data really corresponds to surface-related bands because the local-orbital occupations show major contribution from the Bi atoms at the corresponding theoretical bands. The experimental energy values of the $s2$ near the Γ point are about 0.1 eV larger than the corresponding theoretical energies at maximum. This is probably partially due to the uncertainties described above. Only the $s2$ dispersion is clear: it shows the

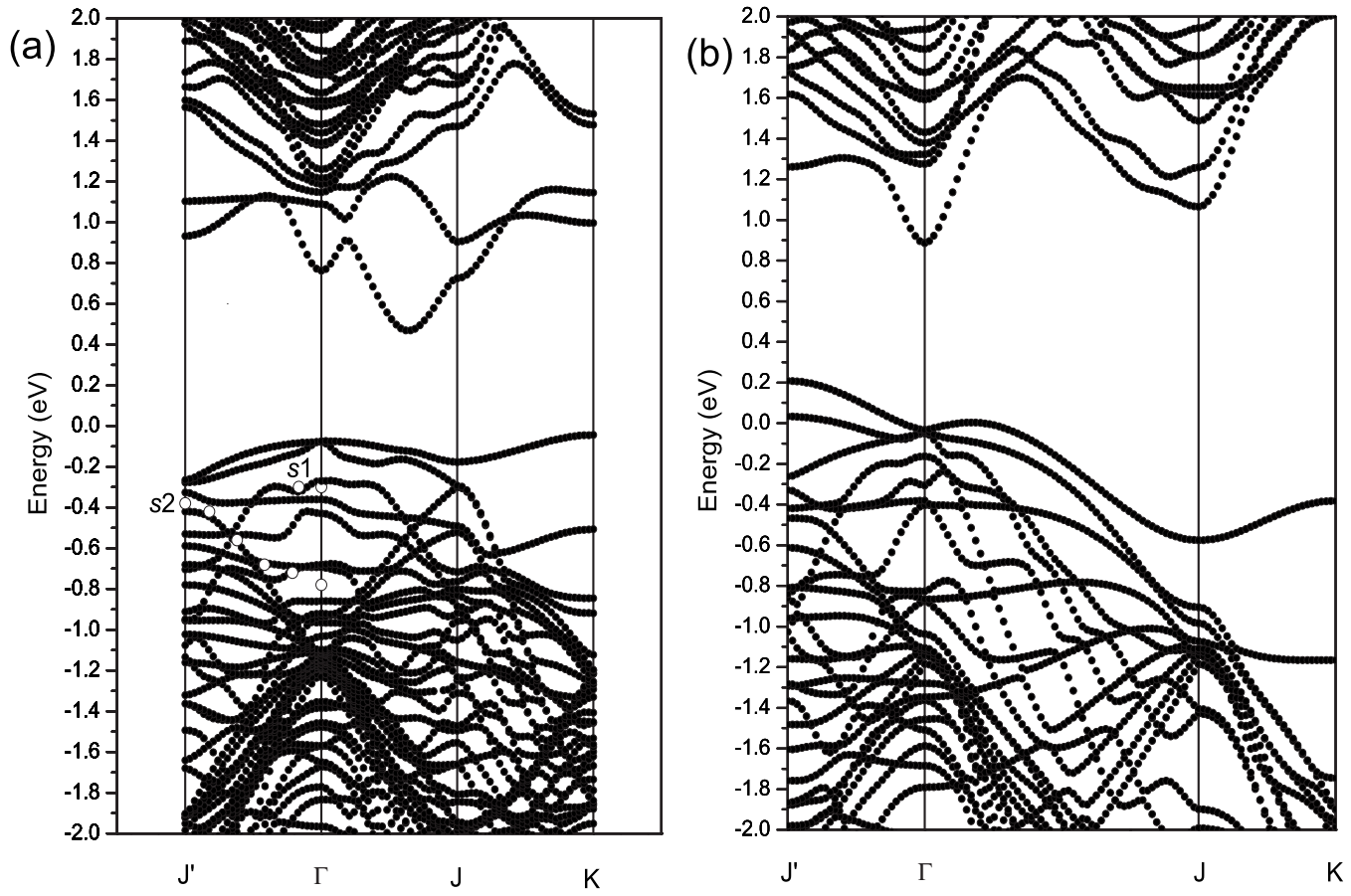

FIG. 6. (a) Theoretical and experimental band structures along the main symmetry directions of the Bi/GaAs(100)(2×1)-sBiAs reconstruction. The 0 eV level is set at the bottom of the energy gap. The solid circles denote the theoretical results, whereas the open circles denote the experimental results. (b) Theoretical band structure along the main symmetry directions of the hypothetical As/GaAs(100)(2×1)-BiBi reconstruction. The theoretical Fermi level is set at 0 eV.

twofold periodicity in the [0−11] azimuth, in good consistency with the dimerization of the surface structure along this direction. The *s*2 closely resembles the surface state found previously on the As-stabilized and Sb-stabilized GaAs(100)(2×4) surfaces.[26,39] One can easily notice two surface bands, which cause the metallicity of the BiBi reconstruction, in the Γ-*J* direction. Furthermore, three surface states are found at the *K* symmetry point. For example, there are three surface states at the *K* point of the BiBi reconstruction at energies of −0.67, −0.76, and −1.51 eV, which have a strong contribution from the p_{100} orbitals. The orbital character (p_x, p_y, p_z) of the several surface-related bands is strongly varied along the symmetry directions. (This is especially true for the surface-related bands, which overlap bulk bands.) There are, however, exceptions. For example, the surface band along the Γ-*J*′ direction of the BiBi reconstruction at the energy of 0.6 eV originates mostly from the Bi *p* orbitals perpendicular to the direction of the dimerization and the corresponding *p* orbitals of the underlying Ga atoms. Furthermore, the surface character of the band can also change. For example, the surface state at energy of −1.51 eV at the *K* point of the BiBi reconstruction loses its surface nature around the middle point of the *J*-*K* line.

The DOS of the Bi/GaAs(100)(2×1) is decreased at the Fermi energy compared to the corresponding values of the hypothetical Sb/GaAs(100)(2×1) and As/GaAs(100)(2×1), which leads to the formation of the pseudogap at the Fermi energy (Fig. 7).[10] This is attributed to the symmetry change in the surface bonds due to the large size of the Bi atom, which results in differed orbital characters of the occupied bands near the Fermi energy.[10] Figure 6(b) represents the band structure of the As/GaAs(100)(2×1), which differs considerably from the band structure of the Bi/GaAs(100)(2×1). There are two surface bands, which are predominantly of the p_{011} character, near the bulk VBM at the *J*′ symmetry point (at energies of 0.03 and 0.21 eV). The corresponding bands are shifted to considerably higher energies at the Bi-stabilized surface in the Γ-*J*′ symmetry direction. On the other hand, the topmost (occupied) surface band along the *J*-*K* symmetry direction (which is the band having the energy of 0.21 eV at the *J*′ point on the As/GaAs) having strong contribution from the p_{100} orbitals is deepened in energy. It is proposed that this contributes substantially to the stabilization of the Bi/GaAs(100)(2×1). This conclusion is supported by the charge-density plots of the topmost occupied surface band in the *J*-*K* symmetry direction for the Bi/GaAs(100)(2×1) and As/GaAs(100)(2×1) presented in Fig. 8, which show that the charge of this band is more concentrated between Bi and Ga atoms than As and Ga atoms, and therefore, more bonding on the Bi-stabilized sur-

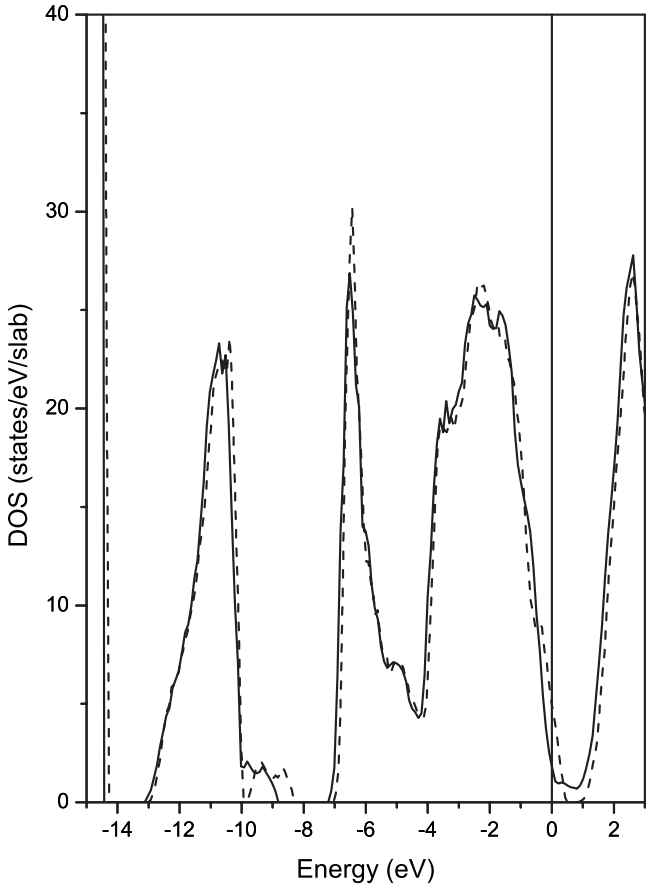

FIG. 7. Theoretical density of states of the Bi/GaAs(100)(2 $\times$1)-BiBi (solid line) and the hypothetical As/GaAs(100)(2 $\times$1)-AsAs (dashed line). The theoretical Fermi level is set at 0 eV.

face. These effects are due to the increase in the vertical positions of the Bi dimer atoms compared to the underlying Ga atoms, which leads, e.g., to the considerably smaller angle between the backbonds (90.39° on the Bi/GaAs and 106.02° on the As/GaAs). The smaller angle between backbonds may lead to smaller Coulomb repulsion between backbond charge and dangling bond charge,[40,41] which contributes to the energy shifts of the considered bands. These effects really are due to the geometry of the surface structure because Bi atoms at the As positions of the As/GaAs(100)(2 $\times$1) lead to a band structure, which is very similar to the band structure of the As/GaAs(100)(2 $\times$1) (same reasoning applies also to the replacement of Bi atoms by As atoms). Thus, the atom size effect explains the band-derived contribution to the stabilization of the Bi/GaAs(100)(2 $\times$1) and the formation of the pseudogap.

B. Atomic models and SCLSs of the Bi/GaAs(100)(2 $\times$4)-α2

Concerning the Bi/GaAs(100)(2 $\times$4) surface, we have examined six different (2 $\times$4)-α2 structures. These include the 2BiBi and BiBi, shown in Figs. 1(d) and 1(e) and calculated recently,[10] and their modifications in which the first layer and/or third layer dimers are replaced by mixed Bi-As ones. The different configurations are listed in Table I showing the SCLS results, to which we return below. Our total-

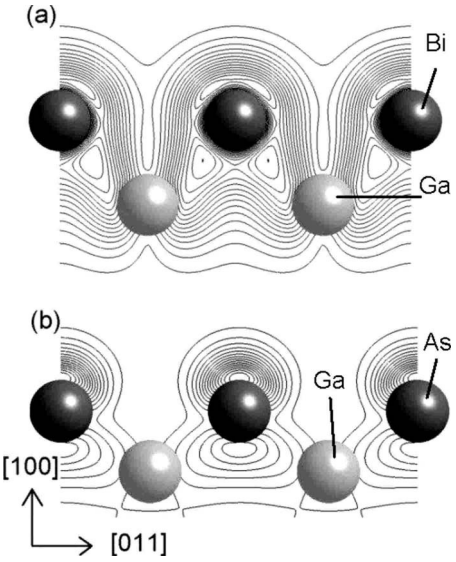

FIG. 8. Valence electronic charge-density plots of the topmost occupied band along the *J*-*K* symmetry direction for the (a) Bi/GaAs(100)(2 $\times$1) and (b) hypothetical As/GaAs(100)(2 $\times$1) in plane perpendicular to the direction of dimer bonds through a Bi (As) atom. The Bi and As atoms are shown by black spheres and the Ga atoms are shown by gray spheres.

energy calculations show that the (2 $\times$4)-α2-2BiBi and BiBi phases are stable, as found recently.[10] In addition to these, two mixed (2 $\times$4)-α2 phases, (i) the Bi-Bi dimer in the first layer and the Bi-As dimer in the third layer and (ii) the Bi-As dimer in the first layer and the Bi-Bi dimer in third layer, are found to be stable. The results presented below for the Bi/GaAs(100)(2 $\times$4) are compatible with the existence of these stable models.

Figure 9 shows the As 3*d* and Ga 3*d* spectra from the Bi/GaAs(100)(2 $\times$4) surface. Their fitting was done with the minimum number of SCLS. The minimum number of different emission components, which was deduced from asymmetries or shoulders of the spectral line shapes, was included in the fitting procedure. It was done using the Voigt-profile peaks with the standard methods. The background of the spectra was subtracted by the Shirley method. The Lorentzian width (LW), spin-orbit splitting (SOS), and branching ratio (BR) (see Fig. 9) were input parameters. In contrast, the Gaussian width and SCLSs were taken as a result of a proper fit. As can be seen in Table I, the SCLS found from spectra agree with those calculated for the various (2 $\times$4)-α2 structures, except for the largest positive binding-energy (BE) shift calculated for both the As 3*d* and Ga 3*d*. This discrepancy is most likely due to our fitting procedure where the minimum number of the components were included. Thus, it is reasonable that we could not deduce all existing components from the pure line shape. Indeed, the correspondence between the fit and the experimental results is not so good, especially for the high binding-energy side of the Ga 3*d* SCLS. Therefore, the strength of the theory is to reveal the number of the SCLS components and their atomic origins, as shown previously.[38]

The Bi 5*d* emission from the Bi/GaAs(100)(2 $\times$4) surface includes at least two components, *S*1 and *S*2, as can be

TABLE I. Measured surface core-level shifts (SCLS in eV) from the Bi/GaAs(100)(2×4) surface and calculated SCLS for the different Bi/GaAs(100)(2×4)-α2 structures with the different group V dimers in the first (topmost) and third atomic layers. Negative values indicate smaller BE as compared to the reference, which is the bulk BE for the Ga 3*d* and As 3*d* levels. For calculated Bi SCLS, 0 eV level is the electron BE in the topmost dimer of the Bi/GaAs(100)(2×4)-α2-2BiBi structure (i.e., first layer: Bi-Bi and third layer: Bi-Bi). In the measured Bi 5*d* spectrum, *S*2 is set at 0 eV.

Bi/GaAs(100)(2×4)	Bi 5*d*	Ga 3*d*	As 3*d*
Measured SCLS	−0.49 (*S*1), 0 (*S*2)	−0.23 (*S*1), +0.25 (*S*2)	−0.35 (*S*1), −0.16 (*S*2), +0.17 (*S*3)
Calc.: (2×4)-α2 (2BiBi in Fig. 1) 1.layer:Bi-Bi, 3.layer:Bi-Bi	−0.44, 0	−0.15, −0.12, +0.28, +0.50	−0.18, +0.16, +0.29
Calc.: (2×4)-α2 1.layer:Bi-Bi, 3.layer:Bi-As	−0.36, −0.01	−0.18, +0.26, +0.60	−0.25, −0.18, +0.16, +0.30
Calc.: (2×4)-α2 (BiBi in Fig. 1) 1.layer:Bi-Bi, 3.layer:As-As	−0.03	−0.16, −0.12, +0.27, +0.50	−0.35, −0.18, +0.15, +0.31
Calc.: (2×4)-α2 1.layer:Bi-As, 3.layer:Bi-Bi	−0.44, +0.09	−0.15, −0.11, +0.27, +0.50	−0.20, +0.16, +0.32
Calc.: (2×4)-α2 1.layer:Bi-As, 3.layer:Bi-As	−0.35, +0.08	−0.17, −0.11, +0.26, +0.50	−0.34, −0.21, +0.14, +0.34
Calc.: (2×4)-α2 1.layer:Bi-As, 3.layer:As-As	+0.05	−0.18, −0.13, +0.25, +0.49	−0.24, +0.17, +0.33

found in Fig. 10. Comparison with the calculated SCLS in Table I straightforwardly leads to the conclusion that there are Bi atoms in both the first and third layer dimer sites on the Bi/GaAs(100)(2×4) surface. Here, it is worthy to note that we tested the fitting of the As spectrum (not shown) using the calculated SCLSs in Table I and compared it with the fitting of the As 3*d* spectrum of the clean GaAs(100)(2×4) shown in Ref. 38 in Fig. 3 (T=465 °C). The comparison showed that the relative intensities of the SCLS components, contributed by the first and third layer As dimers, decreased on the Bi/GaAs(100)(2×4) surface as compared to the relative intensities of the corresponding components of the clean surface spectrum, in good consistency with the above finding. These results allow us now to confirm the previous tentative suggestion according to which the two Bi SCLS, observed on the various Bi/III-V(100)(2×4) surfaces, arise from the first and third layer dimers.[27,28] Furthermore, our calculations justify the assignment according to which the SCLS at the higher BE (e.g., the present *S*2) is caused by the first layer dimers and the other SCLS at the lower BE (e.g., the present *S*1) is caused by the third layer dimers. This assignment is consistent with the present (Fig. 10) and former findings,[27,28] which show that the higher BE SCLS is more surface sensitive in the measurements than the lower BE component (and therefore is originated from the atoms closer to vacuum). Our calculations show that the

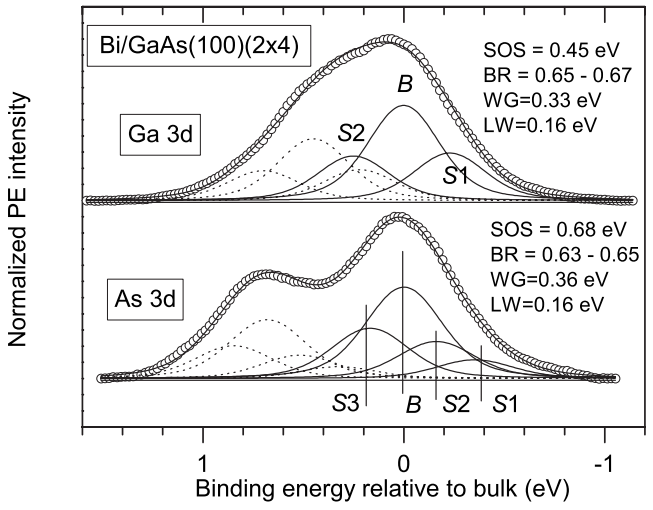

FIG. 9. Fitted As 3*d* and Ga 3*d* spectra measured from the Bi/GaAs(100)(2×4) surface. GW, LW, SOS, and BR are shown. The $d_{5/2}$ peaks of the bulk (*B*) and surface (*S*) doublets are shown by solid lines, whereas the dotted lines represent the corresponding $d_{3/2}$ components. The photon energy and photoelectron emission angle from the normal are 90 eV and 0°, correspondingly.

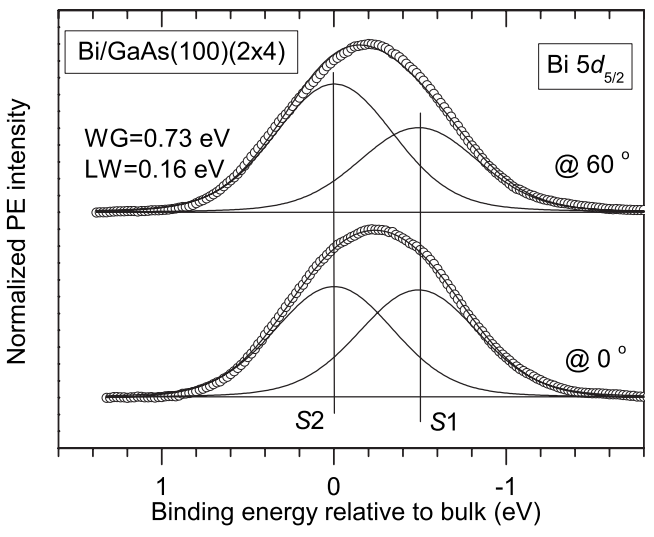

FIG. 10. Fitted Bi $5d_{5/2}$ peaks measured from the Bi/GaAs(100)(2×4) surface. GW, LW, and emission angles are shown. The photon energy is 90 eV.

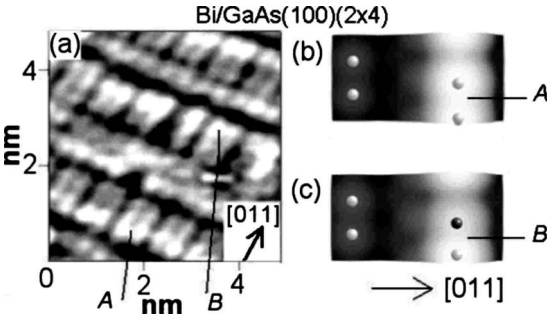

FIG. 11. (a) Filled-state STM image of the Bi/GaAs(100)(2 $\times$4); tunneling current I=0.42 nA and voltage V=2.49 V. (b) Calculated filled-state (2.49 V) image of the Bi/GaAs(100)(2$\times$4)-α2 structure, which includes Bi-Bi dimers in both the first and third layers. The Bi dimer atoms are shown by gray spheres. (c) Calculated filled-state (2.49 V) image of the Bi/GaAs(100)(2$\times$4)-α2 structure, which includes a Bi-As dimer in the first layer and a Bi-Bi dimer in the third layer. The Bi-As dimer is buckled by 0.27 Å, and the Bi atom locates higher (and is more white) than the As atom. The Bi dimer atoms are shown by gray spheres and the As dimer atom by a black sphere.

same assignment is applicable also for the Sb/III-V(100)(2 $\times$4) surfaces showing similar two Sb SCLS components. The BE difference between $S1$ and $S2$ is, e.g., exactly the same on the Sb/GaAs(100)(2$\times$4)-α2-2SbSb as on the Bi/GaAs(100)(2$\times$4)-α2-2BiBi, i.e., 0.44 eV. The first layer Bi dimer atoms lose locally slightly more electrons to vacuum than the third layer Bi dimer atoms, which contributes to the larger BE of the first layer atoms. However, one should note that differences in the interatomic (Madelung) potentials of the considered atoms probably also contribute to the BE differences.

The Gaussian width (GW) of the Bi 5d components is clearly (about twice) larger than the GW of the As 3d and Ga 3d components on the Bi/GaAs(100)(2$\times$4) although these spectra were measured with the same instrumental resolution (see Figs. 9 and 10). This suggests that the Bi/GaAs(100)(2$\times$4) surface includes more than one phase because the presence of several phases causes a variation in the Bi 5d BE of the two main peaks $S1$ and $S2$, as can be found in Table I, and thus the broadening of the Bi peaks. That is, each Bi peak ($S1$ and $S2$) includes most likely two or more peaks which cannot be resolved in the line-shape analysis. The STM image of the Bi/GaAs(100)(2$\times$4) in Fig. 11(a) gives a further support to the presence of both the Bi-Bi and Bi-As dimers. This STM image was taken on the surface which consisted of both the (2$\times$4) and (2$\times$1) areas. Based on the calculated images in Figs. 11(b) and 11(c) for the (2$\times$4)-α2 structures, which include the first layer Bi-Bi and Bi-As dimers, respectively, we propose that the feature A in Fig. 11(a) arises from the Bi-Bi dimer and the feature B arises from the Bi-As dimer. In passing, a local β3-like[42] defect structure with two third layer dimer rows is seen in the measured image between features A and B. The calculated geometries show that the mixed Bi-As dimers are buckled by 0.27 Å and that the Bi atom locates higher (is brighter) than the As atom.

C. Subsurface stress and relative stabilities

Finally, we discuss the reason for the stability of the Bi/III-V(100)(2$\times$4)-α2 over $-$(2$\times$4)-β2 structure. The atoms of group III in the second layer of the (2$\times$4) structures can relax in the [011] direction (the direction perpendicular to the Bi dimer bonds) because the first and second layers are not full. Since the Bi atom is large, it causes a strong relaxation of the second layer group III atoms in the direction perpendicular to the dimer bonds and therefore supposedly subsurface stress. Thus, it is energetically more favorable to place one of the Bi dimers of the (2$\times$4)-β2 to the third layer [(2$\times$4)-α2-2BiBi] than to keep two Bi dimers in the first layer [(2$\times$4)-β2]. We test our hypothesis by calculating the total energies of the GaAs(100)-(2$\times$4)-α2-BiBi, $-$(2 $\times$4)-α2-2BiBi, and $-$(2$\times$4)-β2-BiBi surfaces from which the first and third layer Bi and As dimers are removed and the remaining atoms are kept in the relaxed positions (each resulting system has the same amount of atoms of the same types). These calculations are performed also for the corresponding Sb-stabilized and As-stabilized GaAs(100)(2$\times$4) surfaces. It is found that the total energy of the dimer-free (2$\times$4)-β2 is much higher relative to the dimer-free (2 $\times$4)-α2-VV and (2$\times$4)-α2-2VV (about 0.3 eV/slab) if Bi-stabilized surfaces are compared to the As-stabilized surfaces. The results for the Sb-stabilized surfaces are in between the results of the Bi-stabilized and As-stabilized surfaces but closer to the Bi case. These results support the above hypothesis. The found trend is in accordance with the calculated surface energies for the Bi-stabilized, Sb-stabilized and As-stabilized GaAs(100) surfaces. The (2 $\times$4)-β2-BiBi is not stable in any conditions,[10] but the (2 $\times$4)-β2-SbSb is just in the limit to appear in the theoretical phase diagram, partly because there is a set of chemical potentials (and thus a limited area in the surface phase diagram) for which the (2$\times$4)-β2-SbSb is more stable than the pure surface reconstruction (2$\times$4)-β2-AsAs. As is well known, the (2$\times$4)-β2-AsAs has a large stability area, and this surface is easily found in experiments.

This consideration also reveals additional support for the stability of the Bi-stabilized (2$\times$1) reconstruction discussed in Sec. IV A and in the previous article.[10] It was stated that the driving force for the formation of the Bi-stabilized (2 $\times$1) reconstruction is the strong attractive interaction of the Bi atoms on the nondimerized atom positions (due to the Bi atom size) and that the formation of the pseudogap contributes to the stabilization of the (2$\times$1) reconstruction.[10] We also performed calculations for the Bi-stabilized, Sb-stabilized, and As-stabilized (2$\times$1) reconstructions from which the Bi, Sb, and As dimers were removed. In this case the Bi and Sb dimer-free structures have lower total energies than the As dimer-free surface. We propose that this is due to distorted bonds between the second (Ga) and the third (As) layers on the As-stabilized surface, which may also be related to the subsurface stress. In the (2$\times$1) structure the adsorbant cannot induce relaxation in direction perpendicular to the dimer bond because the first and second layers are full, and therefore the case is essentially different from that of the (2$\times$4) reconstruction discussed above. However, the second layer Ga atoms are slightly relaxed in direction parallel to the

dimer bond. This relaxation is strongest for the As-stabilized surface because the As-As dimer has the shortest dimer bond length. On the other hand, this rearrangement of the second-layer Ga atoms is smallest for the Bi-stabilized surface (total energy of the Sb-stabilized surface is very close) contributing to the relatively low total energy. Again, this is an atom size effect.

V. CONCLUSIONS

The complementary photoemission data and the theoretical band structures support the presence of the Bi/GaAs(100)(2×1) surfaces and the stabilizing mechanisms found recently.[10] It is shown, especially, that Bi adsorption induces energy shifts of the predominantly adsorbate-derived group of bands in different symmetry directions which consequently contribute to the stabilization of the peculiar Bi/GaAs(100)(2×1) reconstruction and the formation of the pseudogap. The calculated SCLS values for various Bi/GaAs(100)(2×4)-α2 structures allow us now to resolve the previous puzzle related to the atomic origins of two SCLS components in the Bi 5*d* emission of the Bi/III-V(100)(2×4) surfaces. Our results confirm that the Bi 5*d* SCLS at the higher BE is caused by the first layer dimers and the other SCLS at the lower BE is caused by the third layer dimers. [The same assignment can be applied also to the corresponding Sb 4*d* SCLS of the Sb/III-V(100)(2×4).] Combining total-energy results, the experimental and theoretical core-level, and STM data, we propose that the asymmetric Bi-As dimers are building blocks of the Bi/GaAs(100)(2×4) surface, in addition to the symmetric Bi-Bi dimers. The rearrangement of the subsurface layers due to the adsorbant atom size and the geometry of the reconstruction leads to the absence of the Bi/III-V(100)(2×4)-β2 reconstruction. The same kind of subsurface relaxation in different direction also contributes to the stabilization of the Bi/III-V(100)(2×1). All effects responsible for the stabilization of the Bi/GaAs(100)(2×1) are shown to be due to the large size of the Bi atom relative to the size of the As atom.

ACKNOWLEDGMENTS

We thank H. Ollila and the MAX-laboratory staff for assistance. This work has been supported in part by the Academy of Finland Grant No. 122743 (P.L.). Three of us would like to acknowledge financial support by the EC Access to Research Infrastructure Program (ARI) (P.L., M.A.-T., and N.R.). Financial support from the Swedish Research Council and the Swedish Foundation for Strategic Research (L.V., S.M., and B.J.) and from the Hungarian Scientific Research Fund under Grant No. T048827 (J.K. and L.V.) is also acknowledged. The calculations were performed using the facilities of the Finnish Centre for Scientific Computing (CSC) and the Mgrid project (Turku, Finland).

*Authors to whom correspondence should be addressed. marko.punkkinen@utu.fi

†pekka.laukkanen@utu.fi

[1] J. K. Shurtleff, R. T. Lee, C. M. Fetzer, and G. B. Stringfellow, Appl. Phys. Lett. **75**, 1914 (1999).

[2] M. R. Pillai, S. S. Kim, S. T. Ho, and S. A. Barnett, J. Vac. Sci. Technol. B **18**, 1232 (2000).

[3] G. Feng, K. Oe, and M. Yoshimoto, J. Cryst. Growth **301-302**, 121 (2007).

[4] B. Fluegel, S. Francoeur, A. Mascarenhas, S. Tixier, E. C. Young, and T. Tiedje, Phys. Rev. Lett. **97**, 067205 (2006).

[5] X. Lu, D. A. Beaton, R. B. Lewis, T. Tiedje, and M. B. Whitwick, Appl. Phys. Lett. **92**, 192110 (2008).

[6] S. Francoeur, S. Tixier, E. Young, T. Tiedje, and A. Mascarenhas, Phys. Rev. B **77**, 085209 (2008).

[7] M. Ahola-Tuomi, P. Laukkanen, R. E. Perälä, M. Kuzmin, J. Pakarinen, I. J. Väyrynen, and M. Adell, Surf. Sci. **600**, 2349 (2006).

[8] P. Laukkanen, J. Pakarinen, M. Ahola-Tuomi, M. Kuzmin, R. E. Perälä, I. J. Väyrynen, A. Tukiainen, J. Konttinen, P. Tuomisto, and M. Pessa, Phys. Rev. B **74**, 155302 (2006).

[9] P. Laukkanen, M. Ahola-Tuomi, M. Kuzmin, R. E. Perälä, I. J. Väyrynen, A. Tukiainen, J. Pakarinen, M. Saarinen, and M. Pessa, Appl. Phys. Lett. **90**, 082101 (2007).

[10] P. Laukkanen, M. P. J. Punkkinen, H.-P. Komsa, M. Ahola-Tuomi, K. Kokko, M. Kuzmin, J. Adell, J. Sadowski, R. E. Perälä, M. Ropo, T. T. Rantala, I. J. Väyrynen, M. Pessa, L. Vitos, J. Kollár, S. Mirbt, and B. Johansson, Phys. Rev. Lett. **100**, 086101 (2008).

[11] C. B. Duke, Chem. Rev. (Washington, D.C.) **96**, 1237 (1996).

[12] D. J. Chadi, J. Vac. Sci. Technol. A **5**, 834 (1987).

[13] M. D. Pashley, Phys. Rev. B **40**, 10481 (1989).

[14] J. Neugebauer, T. K. Zywietz, M. Scheffler, J. E. Northrup, H. Chen, and R. M. Feenstra, Phys. Rev. Lett. **90**, 056101 (2003).

[15] D. K. Biegelsen, R. D. Bringans, J. E. Northrup, and L. E. Swartz, Phys. Rev. B **41**, 5701 (1990).

[16] J. E. Northrup and S. Froyen, Phys. Rev. B **50**, 2015 (1994).

[17] T. Hashizume, Q.-K. Xue, A. Ichimiya, and T. Sakurai, Phys. Rev. B **51**, 4200 (1995).

[18] G. P. Srivastava and S. J. Jenkins, Phys. Rev. B **53**, 12589 (1996).

[19] Q.-K. Xue, T. Hashizume, and T. Sakurai, Prog. Surf. Sci. **56**, 1 (1997).

[20] W. G. Schmidt, F. Bechstedt, N. Esser, M. Pristovsek, Ch. Schultz, and W. Richter, Phys. Rev. B **57**, 14596 (1998).

[21] V. P. LaBella, H. Yang, D. W. Bullock, P. M. Thibado, P. Kratzer, and M. Scheffler, Phys. Rev. Lett. **83**, 2989 (1999).

[22] M. Göthelid, Y. Garreau, M. Sauvage-Simkin, R. Pinchaux, A. Cricenti, and G. Le Lay, Phys. Rev. B **59**, 15285 (1999).

[23] F. Grosse, W. Barvosa-Carter, J. Zinck, M. Wheeler, and M. F. Gyure, Phys. Rev. Lett. **89**, 116102 (2002).

[24] W. G. Schmidt, Appl. Phys. A: Mater. Sci. Process. **75**, 89 (2002).

[25] A. Ohtake, Phys. Rev. B **74**, 165322 (2006).

[26] P. Laukkanen, R. E. Perälä, R.-L. Vaara, I. J. Väyrynen, M. Kuzmin, and J. Sadowski, Phys. Rev. B **69**, 205323 (2004).
[27] P. Laukkanen, M. Ahola, M. Kuzmin, R. E. Perälä, I. J. Väyrynen, and J. Sadowski, Surf. Sci. **598**, L361 (2005).
[28] P. Laukkanen, M. Ahola-Tuomi, J. Adell, M. Adell, K. Schulte, M. Kuzmin, M. P. J. Punkkinen, J. Pakarinen, A. Tukiainen, R. E. Perälä, I. J. Väyrynen, and M. Pessa, Surf. Sci. **601**, 3395 (2007).
[29] D. M. Ceperley and B. J. Alder, Phys. Rev. Lett. **45**, 566 (1980).
[30] J. P. Perdew and A. Zunger, Phys. Rev. B **23**, 5048 (1981).
[31] P. E. Blöchl, Phys. Rev. B **50**, 17953 (1994).
[32] G. Kresse and D. Joubert, Phys. Rev. B **59**, 1758 (1999).
[33] G. Kresse and J. Hafner, Phys. Rev. B **47**, 558 (1993).
[34] G. Kresse and J. Hafner, Phys. Rev. B **49**, 14251 (1994).
[35] G. Kresse and J. Furthmüller, Comput. Mater. Sci. **6**, 15 (1996).
[36] G. Kresse and J. Furthmüller, Phys. Rev. B **54**, 11169 (1996).
[37] K. Shiraishi, J. Phys. Soc. Jpn. **59**, 3455 (1990).
[38] M. P. J. Punkkinen, P. Laukkanen, K. Kokko, M. Ropo, M. Ahola-Tuomi, I. J. Väyrynen, H.-P. Komsa, T. T. Rantala, M. Pessa, M. Kuzmin, L. Vitos, J. Kollár, and B. Johansson, Phys. Rev. B **76**, 115334 (2007).
[39] P. K. Larsen, J. F. van der Veen, A. Mazur, J. Pollmann, J. H. Neave, and B. A. Joyce, Phys. Rev. B **26**, 3222 (1982).
[40] R. D. Meade and D. Vanderbilt, Phys. Rev. Lett. **63**, 1404 (1989).
[41] Y. He and J. G. Che, Surf. Sci. **569**, 176 (2004).
[42] A. Ohtake, Surf. Sci. Rep. **63**, 295 (2008).